ORIGINAL ARTICLE

The El Niño and Southern Oscillation in the historical centennial integrations of the new generation of climate models

**J. -P. Michael · Vasubandhu Misra ·
Eric P. Chassignet**

Abstract   In this study, we compare the simulation of El Niño and the Southern Oscillation (ENSO) in the historical integrations of 17 Coupled Model Intercomparison Project 5 (CMIP5) models with corresponding observations. The mean state and ENSO variations are analyzed in both the atmosphere and ocean and it is found that most of the CMIP5 models exhibit cold (warm) biases in the equatorial (subtropical eastern) Pacific Ocean sea surface temperature that are reminiscent of the split intertropical convergence zone phenomenon found in previous studies. There is, however, a major improvement in the representation of the power spectrum of the Niño3.4 sea surface temperature variations, which shows that, as in the observations, a majority of the models display a spectral peak in the 2–7 year range, have a near-linear relationship with the displacement of the equatorial thermocline and exhibit a robust atmospheric response to ENSO variations. Several issues remain such as erroneous amplitudes in the Niño3.4 sea surface temperature spectrum's peak and a width of the spectral peak that is either too broad or too narrow. It is also seen that most CMIP5 models unlike the observations extend the ENSO variations in the equatorial Pacific too far westward beyond the dateline and there is very little asymmetry in event duration between the warm and cold phases. ENSO variability forces a dominant mode of rainfall variability in the southeastern United States, especially in the boreal winter season. The CMIP5 exhibited a wide range of response in this metric with several displaying weak to nonexistent, some showing relatively strong, and one indicating excessively zonally symmetric teleconnection over the southeastern United States.

Keywords   ENSO · CMIP5 · El Niño · Southern Oscillation · Ocean–atmosphere interaction · Climate · Variability

J.-P. Michael (✉)
Department of Earth, Ocean and Atmospheric Science and Center for Ocean-Atmospheric Prediction Studies, Florida State University, Tallahassee, FL, USA
e-mail: jpmichael@fsu.edu

V. Misra · E. P. Chassignet
Florida Climate Institute, Florida State University, Tallahassee, FL, USA

Introduction

Validating El Niño and the Southern Oscillation (ENSO) in coupled ocean–atmosphere climate models is considered to be vital to understand and build confidence in the fidelity of the model (Guilyardi et al. 2009). This is partly because ENSO is one the best known natural climate variations (Philander 1990), which is relatively well observed (Zebiak and Cane 1987; Battisti 1988; Battisti and Hirst 1989; Hayes et al. 1991; McPhaden 1993; Jin 1997; Neelin et al. 1998) and, in comparison with other natural climate signals, is well understood theoretically (Kirtman 1997; Clarke 2008). There is also a good precedent for ENSO intercomparison studies which have been benchmarking the progress of the global coupled ocean–atmosphere model development (Mechoso et al. 1995; AchutaRao and Sperber 2006; Guilyardi et al. 2012). In the process of this constant engagement of ENSO verification from one generation of models to the other, the community is slowly getting a better comprehension of the metrics that critically evaluate the model simulations (Guilyardi et al. 2009; NRC

◄ Fig. 1 **a** Observed annual mean SST (ERSSTv3b) and annual mean SST errors from, **b** BCC-CSM1-1, **c** CanESM2, **d** CCSM4, **e** CNRM-CM5, **f** CSIRO-Mk3-6, **g** GFDL-CM3, **h** GFDL-ESM2G, **i** GFDL-ESM2 M, **j** GISS-E2-H, **k** GISS-E2-R, **l** HadGEM2-ES, **m** INM-CM4, **n** IPSL-CM5A-LR, **o** MIROC5, **p** MPI-ESM-LR, **q** MRI-CGCM3, and **r** NorESM1-M; the units are in °C. Values significant at 95 % confidence limit are shaded

2010). Most importantly, however, ENSO variations strongly affect the climate variations in the southeastern United States (Ropelewski and Halpert 1987; Kiladis and Diaz 1989; Diaz et al. 2001; Misra and DiNapoli 2012). Therefore, the validation of the ENSO simulation in a climate model is relevant to evaluating its efficacy for use in understanding the southeastern US climate variations and change.

From the first climate model intercomparison study that displayed no ENSO features (Mechoso et al. 1995), there has been a steady, incremental progress in the simulation of ENSO (Guilyardi et al. 2012). One of the significant challenges in improving ENSO representation climate models is that we have not come across a panacea that works universally across all coupled models. For example, several modeling groups have successfully improved the tropical mean state and the ENSO simulation of their climate models by changing one of the following (a) deep convective parameterization scheme in the atmospheric model (Zhang and Wang 2006; Neale et al. 2008), (b) diffusion in the ocean models (Meehl et al. 2001), and (c) resolution of the atmospheric and oceanic models (Gent et al. 2010). However, the same modification in other climate models did not lead to the same improvement and often yielded undesired results (http://www.iges.org/ctbm 05/meetingreport.html). It is important to note that most of these climate models continue to systematically display a

Fig. 2 The annual mean thermocline depth (20 °C isotherm) in meters averaged between 5S-5 N

split intertropical convergence zone (ITCZ) (Mechoso et al. 1995), which is considered to be detrimental to the ENSO simulation. Modest improvements in the intensity of this split-ITCZ bias have been reported in (Zhang and Wang 2006; Neale et al. 2008).

Other common errors in the representation of ENSO in coupled models are an erroneous westward extension of the ENSO variability beyond the dateline, a narrower than observed meridional extent of the equatorial Pacific SST anomalies, and an ENSO which is too periodic and symmetric (AchutaRao and Sperber 2006; Joseph and Nigam 2006). Features of ENSO that are traditionally well represented are the seasonal phase locking of ENSO variability and the teleconnection of ENSO over North America (Misra et al. 2007; Joseph and Nigam 2006).

In this study, we examine the mean state as well as the variations on the ENSO timescales in the historical simulations of the Coupled Model Intercomparison Project 5 (CMIP5) models, which will be used in preparing the International Panel for Climate Change (IPCC) Assessment Report 5 (AR5). It should be noted that the CMIP3 suite of models was used in the preparation of AR4 (Solomon et al. 2007); there was no CMIP4. A brief description of the model output and the validation datasets used in the analysis are provided in the supplementary material. The results are discussed in the following section followed by conclusions in "Summary and conclusion."

Results

Mean state

Several studies (Federov and Philander 2001; Wittenberg et al. 2006) suggest that fidelity of the mean state is critical for successful ENSO simulation. The mean observed SST field (Fig. 1a) shows the equatorial cold tongue off the coast of Peru and the tropical western Pacific warm pool. The replication of this equatorial zonal temperature gradient is important for the coupled feedbacks of the ENSO variations (Clarke 2008). The CMIP5 model SST error fields (Fig. 1b–r) exhibit biases in three areas: a cold bias over the cold tongue in the equatorial Pacific Ocean, a warm bias in the eastern oceans of the subtropical region, and a cold bias in the western portion of the subtropical Pacific Ocean. The annual mean SST errors averaged over these three regions are indicated in Table 2.1[1]. All of these errors were quite prevalent in the CMIP3 models (AchutaRao and Sperber 2006; Capotondi et al. 2006), and unfortunately, these errors are still present in the CMIP5 suite of models. The most extreme cold bias in the
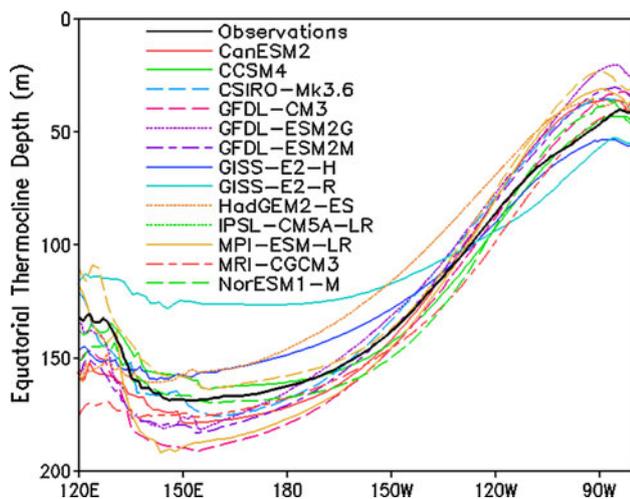
---

[1] See supplementary material for details.

equatorial Pacific is seen in the CSRIO-Mk3.6 (Fig. 1f) and it is the only model to have a cold bias over nearly the entire tropical Pacific basin. However, GISS-E2-H (Fig. 1j) and GISS-E2-R (Fig. 1k) display a widespread warm bias across the eastern oceans, covering even the cold tongue region. In GFDL-CM3 (Fig. 1g), MIROC5 (Fig. 1o), and NorESM1-M (Fig. 1r), the errors at the equator and over the Peruvian coast are comparatively far less but they show significant cold biases in northwestern Pacific. Table 2.1 and Fig. 1c indicate that CanESM2 has the least bias in these three regions.

In Fig. 2, we show the Pacific equatorial cross-section of the mean thermocline depth (defined as the depth of the 20 °C isotherm) averaged between 5°S and 5°N for each of the models overlaid with the depth from the observations-based reanalysis GODAS[*]. It is generally seen that the slope of the thermocline depth is reasonably well captured by the models with deeper (shallower) depths in the western (eastern) equatorial Pacific Ocean. However, the model biases tend to cluster with a majority of the climate models having steeper gradient across equatorial Pacific Ocean. In GISS-E2-R, the slope of the thermocline is relatively weaker than most other models and observations while CCSM4 seems to nearly replicate the zonal gradient of the equatorial Pacific thermocline depth in GODAS. Further information on the climato-logical seasonal cycle of the equatorial Pacific Ocean in the CMIP5 models is provided in the supplementary material.

Spectral analysis

Using the maximum entropy method of order 40 (Ghil et al. 2002), the spectra based on the Niño3.4 SST are shown in Fig. 3; the models have been subdivided into three classes by the strength of the ENSO signal. The Niño 3.4 SST spectral peak of CSIRO-Mk3.6, GFDL-ESM2G, GISS-E2-H, GISS-E2-R, INM-CM4, and IPSL-CM5-LR (Fig. 3a) is broadest of all the other CMIP5 models. Fur-thermore, in this group of models, it may be noted that the amplitude of the spectrum at peak and at the biennial timescale is comparable to the observations. However, four of the models (CSIRO-Mk3.6, GISS-E2-H, GISS-E2-R, INM-CM4, and IPSL-CM5A-LR) in Fig. 3a also exhibit the largest bias in SST (Table 2.1 and Fig. 1). The spectra of BCC-CSM1-1, CanESM2, CNRM-CM5, GFDL-CM3, HadGEM-ES, and MPI-ESM-LR (Fig. 3b) display a very strong ENSO signal (in terms of the amplitude) compared to the observations. Furthermore, with the exception of MPI-ESM-LR, all have a significant secondary peak at around the biennial timescale. Lastly, in Fig. 3c, we show the spectrum of the Niño3.4 SST anomalies from CCSM4, GFDL-ESM2 M, MIROC5, and NorESM1-M, which have

peak variability closer to the observed frequency than other CMIP5 models. However, the power of the ENSO
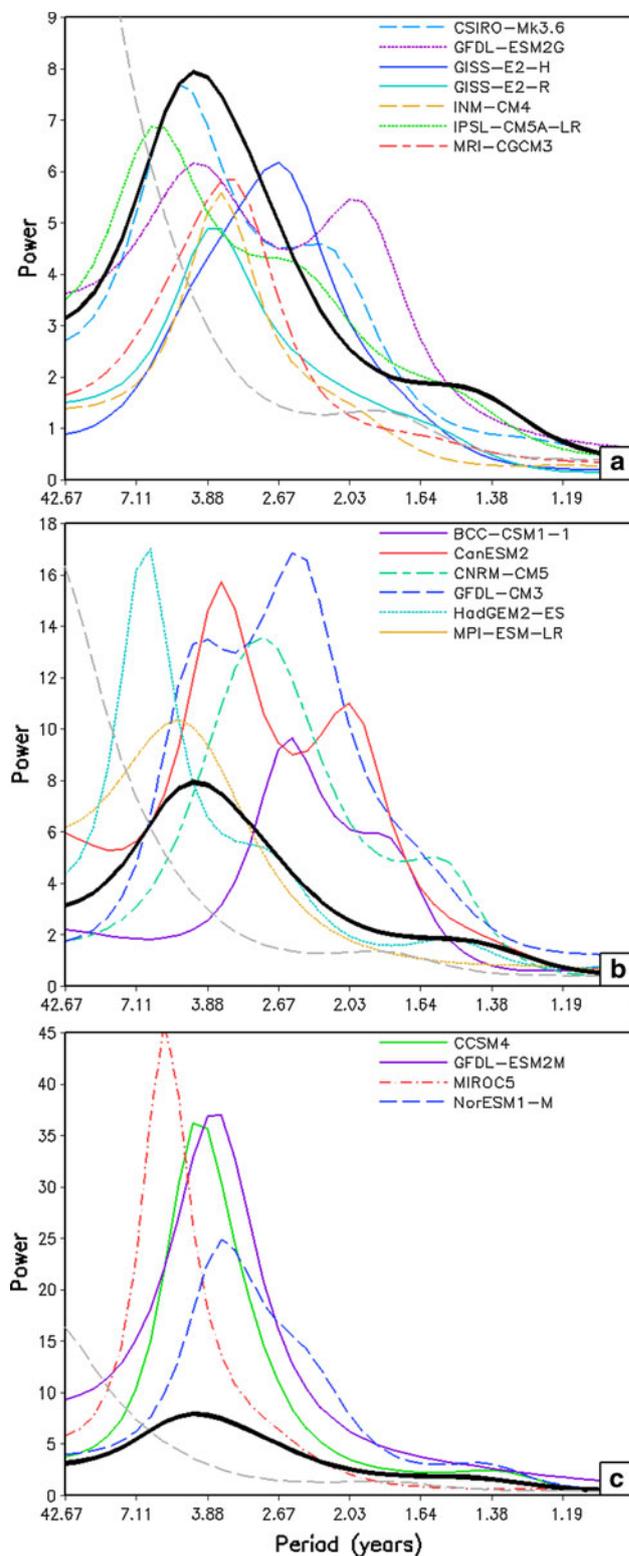
Fig. 3 Sample spectrum of the Niño 3.4 SST using maximum entropy method (Ghil et al. 2002) with observations (ERSSTv3b) in *black* and AR1 model of observations in *gray*

Fig. 4 Lead/lag Niño 3.4 SST regression on equatorial Pacific SST normalized by the standard deviation of the Niño 3.4 SSTs for 17 models. Observations are from ERSSTv3b
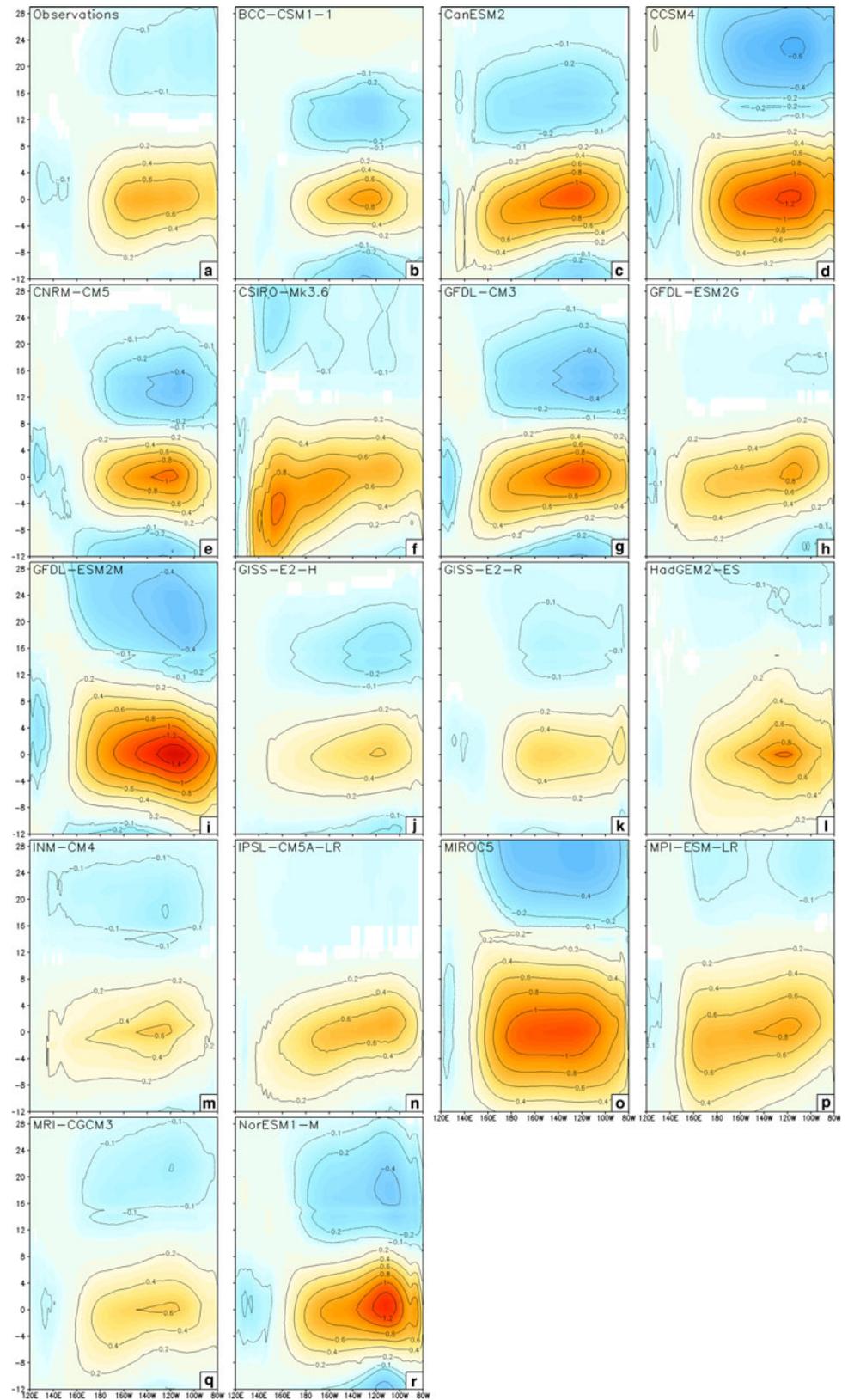
spectrum in this class of models is relatively much higher than any other group of models including that in Fig. 3b. Further, the slender peaks of the spectrum are also indicative of the ENSO events being too periodic in this class of models. The supplementary material further discusses the evaluation of the duration of the ENSO events and the seasonal phase locking feature of ENSO variability. A key feature of the ENSO variations is that it is phase locked with the seasonal cycle of the eastern equatorial Pacific SST (Chang et al. 1995). It is seen that ENSO variability usually peaks near the end of the year when the SST are coolest in the eastern equatorial Pacific. This feature of ENSO is further analyzed in the supplementary material.

Lag/lead relationship with equatorial Pacific

The lag/lead relationship of the Niño3.4 SST anomalies with the SST anomalies over the equatorial Pacific Ocean illustrates the asymmetry between the phases of ENSO, the zonal extent of the ENSO anomalies in the equatorial Pacific, and the period of the ENSO oscillation. Figure 4 shows the normalized lag/lead regressions for the equatorial Pacific SST (averaged between 5°N and 5°S) with Niño3.4 SST anomalies leading (lagging) equatorial Pacific SST anomalies for negative (positive) lags. All the models in Fig. 4, including the observations, show an asymmetry between the ENSO phases, with the amplitude of one phase being relatively stronger than the other. However, a majority of these models fail to show that the duration of one phase is longer than the other with possible exception of GISS-E2-R (Fig. 4k) and MRI-CGCM3 (Fig. 4p). The westward propagation of anomalies is not well simulated by a number of models; CNRM-CM5 (Fig. 4e), GISS-E2-R (Fig. 4k), HadGEM2-ES (Fig. 4l), and MIROC (Fig. 4o) all lack a distinct propagation and GFDL-ESM2 M (Fig. 4i) appears to propagate eastward with time. Another major issue with the CMIP5 simulation is the erroneous westward extension of the SST anomalies beyond the dateline as displayed most acutely by CanESM2 (Fig. 4c), CSIRO-Mk3.6 (Fig. 4f), GFDL-CM3 (Fig. 4g), GFDL-ESM2G (Fig. 4h), GFDL-ESM2 M (Fig. 4i), GISS-E2-H (Fig. 4j), INM-CM4 (Fig. 4m), IPSL-CM5A-LR (Fig. 4m), MIROC5 (Fig. 4o), and MPI-ESM-LR (Fig. 4p). In contrast, some models are unable to get the anomalies far enough to the east near the Peruvian coast (e.g., GISS-E2-H [Fig. 4j], GISS-E2-R [Fig. 4k], INM-CM4 [Fig. 4m], IPSL-CM5A-LR [Fig. 4n], and MRI-CGCM3 [Fig. 4q]). The variations of the eastern equatorial Pacific SST are closely related to the associated variations in the depth of the underlying thermocline (Zelle et al. 2004), which is further discussed in the supplementary material.

Remote ENSO forcing over the Southeastern United States

The midlatitude response as a result of atmospheric waves traversing the great circle from anomalous convection in the equatorial oceans as a consequence of in situ anomalous warm SST has been found to constitute over 50 % of the variance of the boreal winter 200 hPa geopotential heights in some areas of North America (Wallace and Gutzler 1981; Straus and Shukla 2000) including the southeastern United States. As a result of this teleconnection, El Niño (La Niña) winters are typically characterized by wet and cold (warm and dry) winter climate in the southeastern United States.

Figure 5a shows the Boreal winter (DJF) regression of Niño3.4 SST anomalies on precipitation from NCEP-NCAR reanalysis; likewise, Fig. 6a shows the Boreal winter (DJF) regression of Niño3.4 SST anomalies on 200 hPa geopotential height. The observed geopotential height anomaly shows the typical high (over tropical Pacific), low (over Alaska), high (over Canadian Prairies), and low (over southeast United States) associated with warm Niño3.4 SST anomalies that dictate the precipitation pattern of the Southeastern United States in Fig. 5a. Most of the CMIP5 models (Figs. 5b–r, 6b–r) are able to capture some form of this ENSO teleconnection over the Southeastern United States. There are large variations in the response, with several being rather weak (GISS-E2-H [Figs. 5j, 6j], GISS-E2-R [Figs. 5k, 6k]), or nonexistent (GFDL-ESM2G [Figs. 5h, 6h], GFDL-ESM2 M [Fig. 5i]); several being relatively strong (CanESM2 [Figs. 5c,6c], CCSM [Figs. 5d, 6d], CSIRO-Mk3-6 [Fig. 5g], NorESM1-M [Fig. 6r]), and one (INM-CM4 [Fig. 5m, 6m]) being excessively zonally symmetric.

Summary and conclusion

The teleconnection of ENSO variation with the southeast climate variations cannot be understated. It is one of the most well-known teleconnection patterns with warm (cold) ENSO events typically resulting in wet (dry) and cold (warm) winters in the southeastern United States. By analyzing the ENSO fidelity in the twentieth century simulations of these CMIP5 models, we are providing some guidance to potential users who would want to use the results of these models to assess the future impact of climate change on say the local ecology, hydrology, crop yield in the southeastern United States.

In this paper, we have examined the surface and subsurface oceanic variables, the coupled feedbacks, and the atmospheric response associated with ENSO variations in the centennial integrations forced with the time varying

Fig. 5 Regression of Niño 3.4 SST on DJF precipitation anomalies normalized by the standard deviation of the Niño 3.4 SST anomalies for **a** observations (NCEP-NCAR), **b** BCC-CSM1-1, **c** CanESM2, **d** CCSM4, **e** CNRM-CM5, **f** CSIRO-Mk3-6, **g** GFDL-CM3, **h** GFDL-ESM2G, **i** GFDL-ESM2 M, **j** GISS-E2-H, **k** GISS-E2-R, **l** HadGEM2-ES, **m** INM-CM4, **n** IPSL-CM5A-LR, **o** MIROC5, **p** MPI-ESM-LR, **q** MRI-CGCM3, and **r** NorESM1-M. Units are in millimeters per day
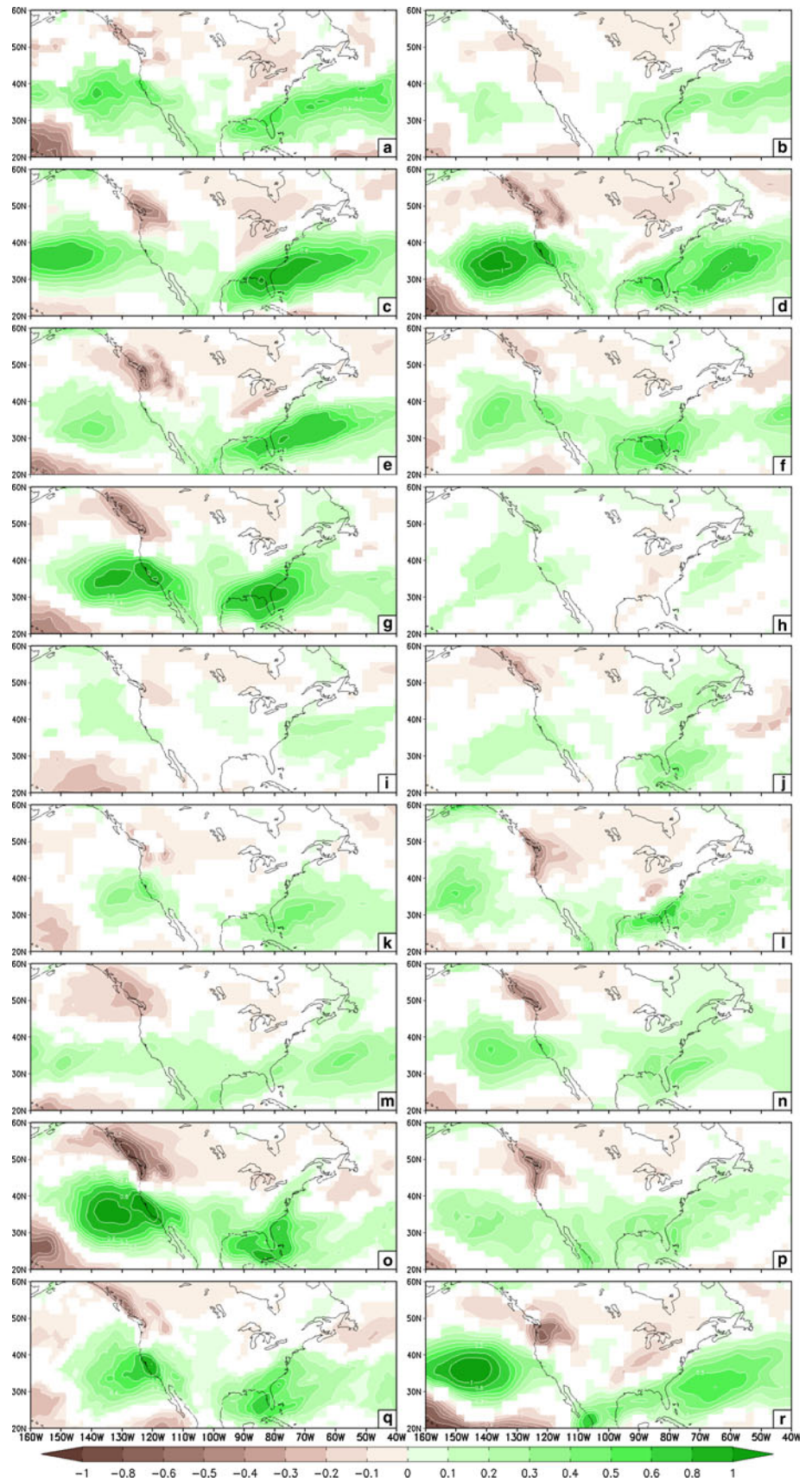
Fig. 6 Linear regression of Niño 3 SST on 200 hPa geopotential height for **a** observations (ERSSTv3b and NCEP-NCAR reanalysis), **b** BCC-CSM1-1, **c** CanESM2, **d** CCSM4, **e** CNRM-CM5, **f** CSIRO-Mk3-6, **g** GFDL-CM3, **h** GFDL-ESM2G, **i** GFDL-ESM2 M, **j** GISS-E2-H, **k** GISS-E2-R, **l** HadGEM2-ES, **m** INM-CM4, **n** IPSL-CM5A-LR, **o** MIROC5, **p** MPI-ESM-LR, **q** MRI-CGCM3, and **r** NorESM1-M. Units are in meters
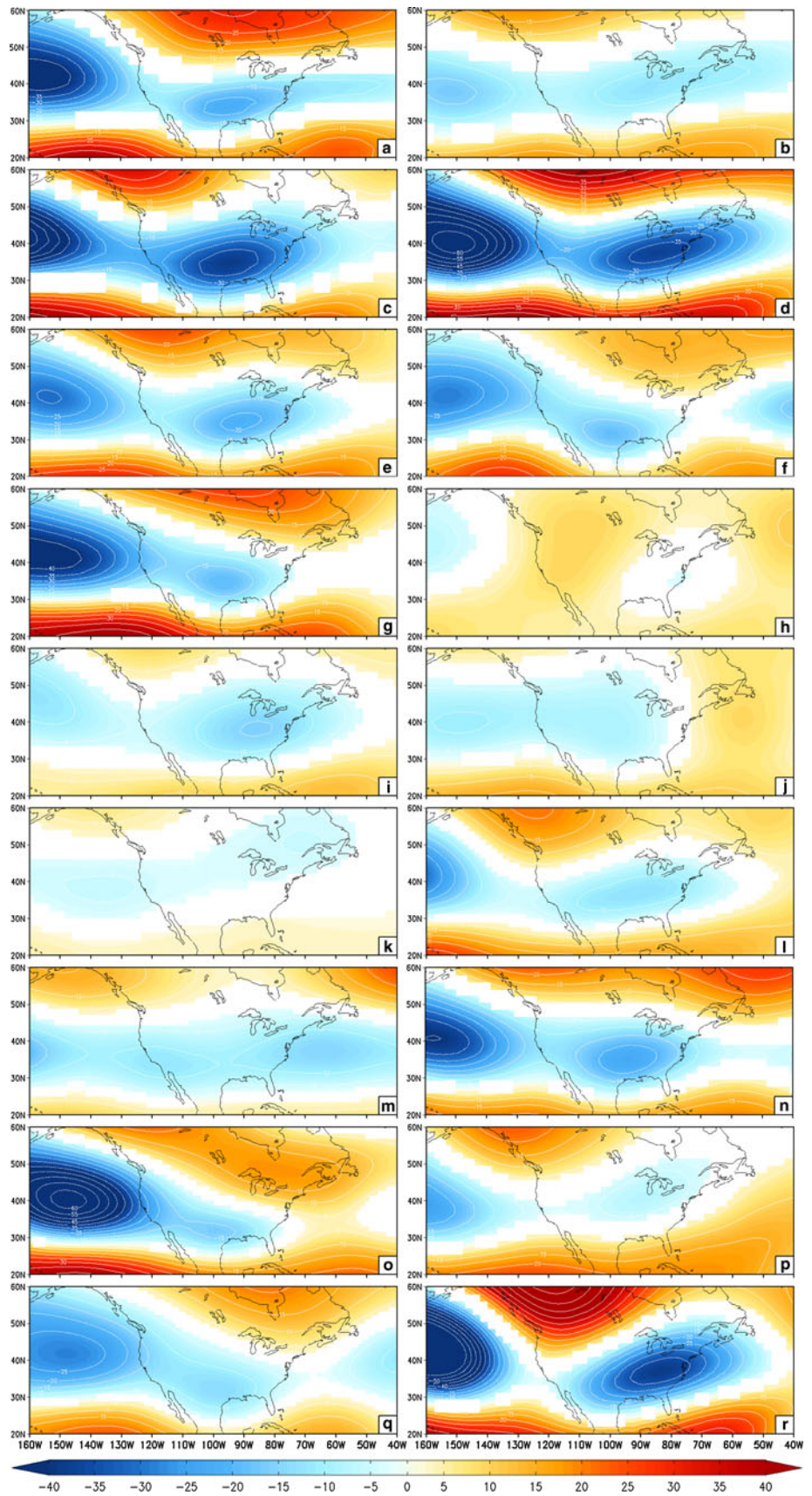
twentieth century emissions of the CMIP5 historical runs. CMIP5 models are part of the latest generation of models that will be extensively analyzed for the forthcoming IPCC AR5. CMIP5 has followed from the CMIP3 suite of models, which was used in IPCC AR4 (Solomon et al. 2007); there was no CMIP4.

Our analysis shows that majority of the CMIP5 models continues to display an erroneous split-ITCZ feature, with a cold SST bias in the equatorial oceans and an overtly active ITCZ just south of the equator. The warm bias in the stratiform regions of the eastern subtropical oceans is also prominent. There was significant diversity in the CMIP5 historical simulation of the ENSO teleconnection with the southeastern US climate. Many models produced geopotential height patterns over North America uncharacteristic of the observed ENSO teleconnection, with either the forced variability being too strong or too weak. These erroneous teleconnections were also reflected in the corresponding ENSO-forced rainfall anomalies over southeastern United States. However, the simulation of the mean state of the equatorial Pacific thermocline is most of the time well represented in the CMIP5 models, with its zonal slope comparable to the GODAS reanalysis. The seasonal cycle of equatorial Pacific SST is also well captured, whereas the seasonality of the coupled feedback between the zonal wind stress and SST shows apparent issues with the models. There is some modest improvement in the power spectrum of the Niño3.4 SST variations from the CMIP3 models, in that the power has increased in several of the models. There are however only a minority of CMIP5 models whose ENSO power spectrum is comparable to the observed spectrum. Lastly, in a majority of the CMIP5 models, the midlatitude atmospheric response to ENSO is quite robust and comparable to observations.

As stated earlier, improving climate models is not a straight forward task especially in a nonlinear model with complex feedbacks. Furthermore, many of the CMIP5 models have introduced more complexities relative to CMIP3 by including interactions with aerosols, land ice, biogeochemical cycle, ecosystem models that could further accentuate the bias through coupled feedbacks. The resolution of the CMIP5 models for these centennial integrations has been raised by at least twofold (and even more in some cases) compared to the CMIP3 models. The community has invested significantly over the years, targeting many of these systematic errors through concerted efforts like the climate process teams in the United States and is actively considering a joint world effort (http://wcrp.ipsl.jussieu.fr/Workshops/ModellingSummit/Documents/FinalSummitStat_6_6.pdf; Shukla et al. 2009) to improve climate models. Validating ENSO simulation seems to be one of the best ways to test the fidelity of a climate simulation given that is relatively well-understood phenomenon, has good observational analysis, and there is a rich historical tradition of verifying ENSO, which has enabled a better understanding of model physics. More specifically, the strong teleconnections of ENSO with the southeastern United States climate makes this validation exercise highly relevant for understanding the reliability of the CMIP5 projections of future southeastern United States climate.

References

AchutaRao Krishna, Sperber KR (2006) ENSO simulation in coupled ocean-atmosphere models: are the current models better? Clim Dyn 27:1–15

Battisti DS (1988) The dynamics and thermodynamics of a warming event in a coupled tropical atmosphere/ocean model. J Atmos Sci 45:2889–2919

Battisti DS, Hirst AC (1989) Interannual variability in the tropical atmosphere-ocean system: influences of the basic state, ocean geometry and nonlinearity. J Atmos Sci 46:1687–1712

Behringer D, Xue Y (2004) Evaluation of the global ocean data assimilation system at NCEP: the Pacific Ocean. Eighth Symposium on Integrated Observing and Assimilation Systems for Atmosphere, Oceans, and Land Surface. AMS 84th Annual Meeting, Seattle, WA, 11–15

Capotondi A, Wittenberg A, Masina S (2006) Spatial and temporal structure of tropical pacific interannual variability in 20th century coupled simulations. Ocean Model 15:274–298

Chang Ping, Ji Link, Wang Bin, Li Tim (1995) Interactions between the seasonal cycle and El Niño-Southern oscillation in an intermediate coupled ocean-atmosphere model. J Atmos Sci 52:2353–2372

Clarke A (2008) An introduction to the dynamics of El Niño and the Southern Oscillation. Academic press, p 324

Diaz HF, Hoerling MP, Eischeid JK (2001) ENSO variability, teleconnections and climate change. Int J Climatol 21:1845–1862

Fedorov AV, Philander SG (2001) A stability analysis of the tropical ocean-atmosphere interactions: bridging measurements of, and theory for El Niño. J Clim 14:3086–3101

Gent PR, Yeager SG, Neale RB, Levis S, Bailey DA (2010) Improvements in a half degree atmosphere/land version of the CCSM. Clim Dyn 34:819–833. doi:10.1007/s00382-009-0614-8

Ghil A et al (2002) Advanced spectral methods for climatic time series. Rev Geophys 40(1):1003. doi:10.1029/2000RG000092

Guilyardi E, Wittenberg A, Fedorov A, Collins M, Wang C, Capotondi A, van Oldenborgh GJ, Stockdale T (2009) Understanding El Niño in ocean-atmosphere general circulation models. Bull Amer Meteor Soc 90:325–339

Guilyardi E, Bellenger H, Collins M, Ferrett S, Cai W, Wittenberg A (2012) A First look at ENSO in CMIP5. Clivar Exchange 59(17):29–32

Guilyiardi E (2006) El Niño mean state-seasonal cycle interactions in a multimodel ensemble. Clim Dyn 26:329–348

Hayes SP, Mangum LJ, Picaut J, Sumi A, Takeuchi K (1991) TAO: a moored array for real-time measurements in the tropical Pacific Ocean. Bull Am Meteorol Soc 72:339–347

Jin Fei–Fei (1997) An equatorial ocean recharge paradigm for enso. Part I: conceptual model. J Atmos Sci 54:811–829

Joseph R, Nigam S (2006) ENSO evolution and teleconnections in IPCCs twentieth-century climate simulations: realistic representation? J. Climate 19:4360–4377

Kalnay E, Kanamitsu M, Kistler R, Collins W, Deaven D et al. (1996) The NCEP/NCAR 40-year reanalysis project. Bull Amer Soc 77:437–471

Kanamitsu M, Ebisuzaki W, Woollen J, Yang S-K, Hnilo JJ, Fiorino M, Potter GL (2002) NCEP-DOE AMIP-II reanalysis (R-2). Bull Amer Met Soc 83:1631–1643

Kiladis GN, Diaz HF (1989) Global climatic anomalies associated with extremes in the Southern Oscillation. J Clim 2:1069–1090

Kirtman BP (1997) Oceanic rossby wave dynamics and the ENSO period in a coupled model. J Clim 10:1690–1704

Li T, Philander G (1996) On the annual cycle in the eastern equatorial pacific. J Clim 9:2986–2998

McPhaden MJ (1993) Trade wind fetch related variations in equatorial undercurrent depth, speed, and transport. J Geophys Res 98:0148–0227. doi:10.1029/92JC02683

Mechoso CR et al (1995) The seasonal cycle over the tropical Pacific in coupled ocean–atmosphere general circulation models. Mon Wea Rev 123:2825–2838

Meehl GA, Gent PR, Arblaster JM, Otto-Bliesner B, Brady E, Craig A (2001) Factors that affect the amplitude of El Niño in global coupled climate models. Clim Dyn 17:515–526

Misra V, DiNapoli SM (2012) Understanding wet season variations over Florida. Clim Dyn 34 doi:10.1007/s00382-012-1382-4

Misra V, L. Marx JLKIII, Kirtnman B (2007) Validating and understanding the ENSO simulation in two coupled climate models. Tellus 59:292–308

Neale RB, Richter JH, Jochum M (2008) The impact of convection on ENSO: from a delayed oscillator to a series of events. J Clim 21:5904–5924

Neelin JD, Battisti DS, Hirst AC, Jin F-F, Wakata Y, Yamagata TS, Zebiak E (1998) ENSO theory. J Geophys Res 103(C7):14261–14290. doi:10.1029/97JC03424

NRC (2010) Assessment of intraseasonal to interannual climate prediction and predictability. The National Academies Press

Philander SG (1990) El Niño, La Niña, and the Southern Oscillation, International Geophysical Series, Vol. 46. Academic Press, pp 293

Ropelewski CF, Halpert MS (1987) Global and regional scale precipitation patterns associated with the El Niño/Southern Oscillation. Mon Wea Rev 115:1606–1626

Shukla J, Hagedorn R, Hoskins B, Kinter J, Marotzke J, Miller M, Palmer TN, Slingo J (2009) Revolution in climate prediction is both necessary and possible: a declaration at the world modeling summit for climate prediction. Bull Amer Met Soc 90:175–178

Smith T, Reynolds R, Peterson TC, Lawrimore J (2008) Improvements to NOAA's historical merged land-ocean surface temperature analysis (1880–2006). J Clim 21:2283–2296

Solomon S et al (2007) Global climate projections. Cambridge University Press, Cambridge, UK

Straus DM, Shukla J (2000) Distinguishing between the SST-forced variability and internal variability in mid-latitudes: analysis of observations and GCM simulations. Quart J Roy Met Soc 126:2323–2350

Taylor KE, Stouffer RJ, Meehl GA (2012) An Overview of CMIP5 and the experiment design. Bull Amer Meteor Soc 93:485–498. doi:10.1175/BAMS-D-11-00094.1

Tziperman E, Cane MA, Zebiak SE (1995) Irregularity and locking to the seasonal cycle in an ENSO prediction model as explained by the quasi periodicity route to chaos. J Atmos Sci 52:293–306

Tziperman E, Zebiak SE, Cane MA (1997) Mechanisms of seasonal—ENSO interaction. J Atmos Sci 54:61–71

Wallace JM, Gutzler DS (1981) Teleconnections in the geopotential height field during the northern hemisphere winter. Mon Wea Rev 109:784–812

Wittenberg AT, Rosati A, Lau N-C, Ploshay JJ (2006) GFDL's CM2 global coupled climate models. Part III: tropical Pacific climate and ENSO. J Clim 19:698–722

Wu R, Kirtman BP (2005) Near-annual SST variability in the equatorial Pacific in a coupled general circulation model. J Clim 18:4454–4473

Xie P, Arkin PA (1997) Global precipitation: a 17-year monthly analysis based on gauge observations, satellite estimates, and numerical model outputs. Bull Amer Meteor Soc 78:2539–2558

Zebiak S, Cane MA (1987) A model for El Niño Southern Oscillation. Mon Wea Rev 115:2262–2278

Zelle H, Appeldoorn G, Burgers G, van Oldenborgh GJ (2004) The Relationship between sea surface temperature and thermocline depth in the eastern equatorial Pacific. J Phy Ocn 34:643–655

Zhang GJ, Wang H (2006) Toward mitigating the double ITCZ problem in NCAR CCSM3. Geophys Res Lett 33:L06709. doi:10.1029/2005GL025229